Construction and Building Materials 158 (2018) 132–140

Contents lists available at ScienceDirect

Construction and Building Materials

journal homepage: www.elsevier.com/locate/conbuildmat

Recycling of desulfurization slag for the production of autoclaved aerated concrete

Ying-Liang Chen [a,*], Ming-Sheng Ko [b], Juu-En Chang [a], Chun-Ta Lin [a]

[a] Department of Environmental Engineering/Sustainable Environment Research Laboratories, National Cheng Kung University, No. 1, University Rd., Tainan 70101, Taiwan
[b] Department of Materials and Mineral Resources Engineering, National Taipei University of Technology, No. 1, Sec. 3, Chunghsiao E. Rd., Taipei 10608, Taiwan

HIGHLIGHTS

- Desulfurization slag has the potential to produce autoclaved aerated concrete.
- The foaming of mortars is retarded due to the insufficient alkalinity.
- Using 0.17 M $NaOH_{(aq)}$ or calcining desulfurization slag can improve mortar foaming.
- Improving foaming results in the products with stable physical properties.
- The formation and morphology of tobermorite are affected by the slag added.

ARTICLE INFO

Article history:
Received 18 August 2017
Received in revised form 26 September 2017
Accepted 26 September 2017

Keywords:
Desulfurization slag
Autoclaved aerated concrete
Tobermorite
Waste recycling

ABSTRACT

The purpose of this study was to reuse desulfurization (De-S) slag in the production of autoclaved aerated concrete (AAC). The non-magnetic fraction of De-S slag is rich in calcium and silicon compounds, and therefore suitable to be an alternative raw material for AAC production. The calcium compounds in the De-S slag used in this study were $Ca(OH)_2$, $CaCO_3$, γ-Ca_2SiO_4, and CaF_2 rather than CaO, and they affected the foaming of AAC mortars due to the insufficient alkalinity. Using 0.17 M $NaOH_{(aq)}$ to replace water or calcining the De-S slag in advance both improved the foaming of mortars, and thus obtained AAC products with stable properties. The formation and morphology of tobermorite in AAC were altered by the addition of De-S slag, probably due to the foreign ions introduced by the slag. The changes in tobermorite should also be related to the decline in the compressive strength of AAC specimens.

1. Introduction

Iron- and steel-making is fundamental to modern society, because it provides the raw materials for buildings, vehicles, and various articles for daily use. In an integrated steel mill, iron is extracted from iron ores and then refined into steel, and at the same time several kinds of slags are generated in different processes. During steelmaking, the liquid iron is treated in order to meet the sulfur specification of steel (typically <0.03%), and a desulfurizer, which is normally composed of lime (CaO, ~90%) and fluorspar (CaF_2, ~10%), is used in the secondary refining process. A layer of slag floating on the liquid iron then forms, and sulfur is removed from the liquid iron by a slag-liquid metal reaction described in Eq. (1) [1,2].

$$Ca^{2+}_{(slag)} + S^{2-}_{(iron)} \rightarrow CaS_{(slag)} \quad (1)$$

Afterwards, the resulting slag, called desulfurization slag (abbreviated to De-S slag), is discharged as a waste and then transported to treatment facilities. Some studies [3,4] reported that De-S slag is primarily composed of excessive lime and entrapped iron, and the desulfurization products (CaS and Al_2O_3), residual fluorspar, and graphite are also present. Although De-S slag normally contains considerable amount of iron and iron oxides, it is not often recycled in steel manufacturing because of the high sulfur content, so reusing DS in cement raw materials, agricultural applications, or wastewater treatments [2,5,6] is a much more feasible and common approach. In Taiwan, about 400,000 tons of De-S slag are generated annually, and most of this is reused in backfilling and controlled low-strength materials, recycling methods that have few economic benefits and could harm the environment.

De-S slag usually has small particle sizes, with Sheng et al. [2] reporting that particles smaller than 0.15 mm accounted for over 60% of the material. Many studies indicate that the major constituents of De-S slag normally include iron (Fe) and iron oxides (FeO, Fe_2O_3, and Fe_3O_4), calcium oxide (CaO), silicon dioxides

* Corresponding author.
E-mail address: roy.yl.chen@gmail.com (Y.-L. Chen).

https://doi.org/10.1016/j.conbuildmat.2017.09.195
0950-0618/

(SiO_2), aluminum oxide, and magnesium oxide (MgO) [3,7,8], and Hwang [9] stated that the metallic iron accounted for 54.1 vol% of the total iron in De-S slag. Ma and Houser [7] reported that the use of weak magnetic separation coupled with selective particle size screening can effectively separate the iron-rich particles from De-S slag, and so obtain a product with low levels of impurities for reuse. After removing iron-rich constituents, the amount of CaO in De-S slag can be increased to 48–69 wt% [8,10], and some researchers use such slag to replace fine aggregate in cement-based concrete materials [10,11]. However, Ho et al. [10] reported that the level of volume expansion of a cement mortar increased along with the amount of De-S slag used, and many studies have suggested that the volume expansion caused by free CaO and MgO from a slag can raise serious concerns with regard to the resulting properties of a construction material [12–14].

While De-S slag has high potential to be reused as a construction material based on its main components, characteristics such as its high powder content and potential volume expansion severely restrict its use. Nevertheless, it could be suitable to reuse De-S slag in the production of autoclaved aerated concrete (AAC), because the disadvantages listed above can be reversed and profitably utilized. AAC is an inorganic building material that is traditionally made from lime powder (5–30 wt%), silica sand (60–70 wt%), cement (5–35 wt%), and water [15–17]. A chemical foaming process is normally used to make AAC lightweight, and an autoclave curing process is employed to drastically increase the mechanical strength of AAC. Under the high-pressure steam conditions in an autoclave, CaO can react with SiO_2 and H_2O to form crystalline hydrates, namely tobermorite, and this reaction contributes to the increase in mechanical strength of AAC [18,19]. Since De-S slag is rich in CaO and SiO_2 and has small particle sizes, it should be able to directly replace lime powder and silica sand to produce AAC, and the free CaO would be consumed during the autoclave curing, thus eliminating the problem of volume expansion. In addition, AAC has several functional properties, such as thermal insulation, fire resistance, and soundproofing, which make it a high-value building material [17], and hence reusing De-S slag to produce AAC can not only promote resource recycling, but also obtain valuable products.

However, several studies have noted that using industrial wastes as AAC raw materials, such as iron and copper tailings, blast furnace slag, and coal bottom ash, may affect the properties and microstructures of the resulting AAC products [15,20–23]. Huang et al. [20] used blast furnace slag and copper tailings as AAC raw materials, and found that some foreign ions, such as Mg and Al, changed the morphology and microstructures of the AAC products. Cai et al. [15] reused iron tailings for AAC production and reported that an increase in the amount of these wastes reduced the compressive strength of AAC, a result that is attributed to the decrease in the amounts of calcium silicate hydrates (C-S-H) and tobermorite. While De-S slag seems suitable for AAC production, little is known about its influence on the process parameters and product properties. Accordingly, the aim of this research is to partially replace lime and silica sand with De-S slag for AAC production, and to examine the effects on the foaming process and the properties of the resulting AAC products.

2. Materials and methods

2.1. Materials

The De-S slag used in this study was generated by an integrated steel mill in Kaohsiung, Taiwan. Hot De-S slag was carried with slag pots and transported to a treatment yard, and then water was poured to cool the slag. Afterwards, the cooled De-S slag was crushed, sieved, and magnetically separated in a slag treatment plant in order to recover any large chunks of iron. The residues from the slag treatment plant were sampled and used as the research subject in this study. The moisture and ash contents, loss on ignition (LOI), magnetic and non-magnetic proportions, particle size distribution, and chemical composition of the treated De-S slag were analyzed immediately after sampling.

2.2. Preparation of AAC specimens

The preparation of AAC specimens included three basic steps, as follows:

(1) Raw material mixing
(CaO, Merck, greater than97%), silica (SiO_2, Alfa Aesar, 99.5%), cement (ordinary Portland cement, ASTM Type I), and the De-S slag were precisely weighed in accordance with the experimental design (Table 1). Because the De-S slag already contained some CaO and SiO_2, the amounts of lime and silica added were adjusted according to the chemical composition of the slag, thus keeping the Ca/Si ratio of the raw mixes constant. The mix proportions of the raw materials of the AAC specimens are listed in Table 1. These raw materials were then put into a steel bowl and mixed with an electric blender until the mix had become homogeneous.

(2) Foaming and pre-curing
(Alfa Aesar, 99.5%) was used as a foaming agent, and the amount added was 0.5 wt%. Water or a NaOH aqueous solution (0.17 M) was then added into the raw mixes at a specific water-solids ratio of 0.70 L/kg, and then blended to mortars as soon as possible using an electric blender at about 120 rpm. The mortar was poured into cast-iron molds (5-cm cubes) and then stood for foaming. After standing for 30 min the foaming of the mortars was finished, and the materials bulging out of the molds were then scraped off. The molds with AAC specimens were immediately put into a moist closet for pre-curing, and the relative humidity and temperature were set at 95% and 25 °C, respectively.

(3) Autoclave curing
After pre-curing in the moist closet for 24 h, the molds were removed and the hardened specimens were obtained. In the final step, an autoclave with a proportional-integral-deriva tive controller was employed to complete the hydration reactions of the hardened specimens, and thus AAC products were obtained. The steam pressure in the autoclave was controlled at 12 atm (the corresponding temperature was about 189 °C), and the curing time was 16 h.

2.3. Material testing and analysis methods

After sampling, the moisture and ash contents and LOI of the De-S slag were immediately analyzed. The LOI value was

Table 1
Mix proportions of raw materials of AAC specimens.

Raw mix	Weight proportion (wt%)			
	Silica	Lime	Cement	De-S slag
Reference	70.0	25.0	5.0	0.0
DS-05	68.1	21.9	5.0	5.0
DS-10	66.2	18.8	5.0	10.0
DS-15	64.3	15.8	4.9	15.0
DS-20	62.4	12.7	4.9	20.0
DS-30	58.6	6.5	4.9	30.0
DS-40	54.8	0.4	4.8	40.0

determined by burning the samples at 950 °C for 3 h. A dry drum magnetic separator (Outokumpu, Model MOS (10) 111–15) was used to separate the magnetic and non-magnetic portions of the De-S slag. The chemical composition of the De-S slags (original, magnetic, and non-magnetic) was analyzed with an inductively coupled plasma-optical emission spectrometer (ICP-OES, PerkinElmer, Optima 2000 DV) following a microwave-assisted acid digestion procedure. The slag samples were digested using a mix acid of nitric, hydrochloric, and hydrofluoric acids at ~175 °C for 24 min with a high-performance microwave digestion unit (Milestone, START D), and the concentrations of elements in the digests were analyzed by means of the ICP-OES. An X-ray diffractometer (XRD, Bruker, D8 Advance) with Cu-Kα radiation was used to characterize the mineralogical composition of the non-magnetic portion of De-S slag. The bulk density and compressive strength of the AAC specimens were determined according to ASTM C1693 [24]. To determine the bulk density of AAC specimens, 5-cm cubic specimens were dried in a ventilated oven at 100–110 °C for at least 24 h to constant weight, and their weight was measured and divided by the volume (125 cm^3) to calculate the bulk density. Thermal analysis was conducted to study the compounds in the AAC specimens using a simultaneous differential scanning calorimetry and thermogravimetric analyzer (DSC-TGA, TA Instrument, SDT 2960). Approximately 20–50 mg of AAC powder was loaded into an alumina crucible for the thermal analysis, and the furnace temperature was programmed to ramp from room temperature to 1000 °C at a heating rate of 10 °C/min under a dynamic nitrogen atmosphere (100 mL/min).

3. Results and discussion

3.1. Characteristics of De-S slag

Fig. 1 presents the particle size distribution of the original De-S slag and its magnetic and non-magnetic proportions in different particle size ranges. The particles larger than 0.85 mm accounted for approximately 60 wt% of the De-S slag, while those smaller than 0.15 mm only accounted for about 13.5 wt%. In terms of magnetic proportion, the particles <0.85 mm contained various amounts of magnetic substances between 23.0 and 31.8 wt%, whereas the particles >0.85 mm had increasing magnetic proportions from 34.9 to 64.7 wt%. These results show that the original De-S slag contained a considerable amount of magnetic substances, although it was already treated with a magnetic separation process in the slag treatment plant, and most of the magnetic substances were distributed in the particles larger than 0.85 mm. Menad et al. [25] reported that the coarse size fractions of the steel slag had higher iron contents because of the residual iron scraps. In this study, the iron-rich portion may be detrimental to the properties of AAC products, and therefore a secondary magnetic separation process was conducted in the laboratory before the further experiments.

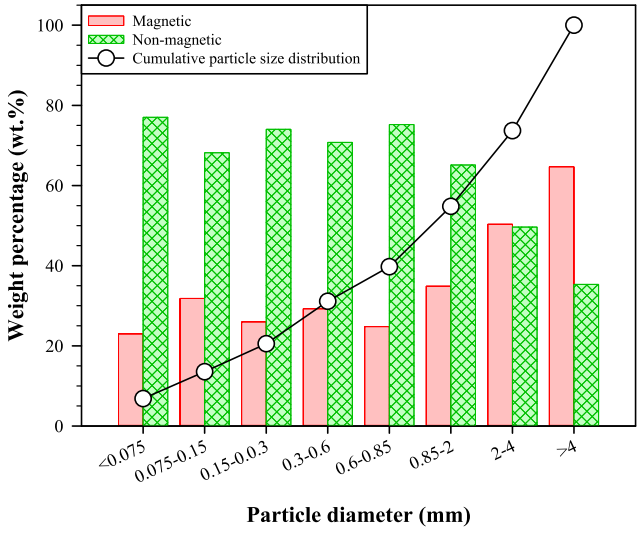

Fig. 1. Cumulative particle size distribution of the De-S slag and its magnetic and non-magnetic proportions in various particle size ranges.

Table 2 shows the characteristics of the original, magnetic, and non-magnetic De-S slags. The moisture content of the original De-S slag was only 9.36 wt%, which should be due to the remaining water during slag cooling. The ash content was 84.31 wt% (93.01 wt% on dry basis), and the LOI was 6.33 wt% (6.99 wt% on dry basis). The LOI of the De-S slag should be attributed to the decomposition of some minerals (e.g. calcium hydroxide and calcium carbonate) and the combustion of the Kish graphite [4]. The characteristics of high ash content and low LOI show that the De-S slag should be suitable for use in the production of inorganic building materials. By conducting a secondary magnetic separation process in the laboratory, the magnetic fraction of the De-S slag was close to 40 wt%. Table 2 also provides the chemical compositions of the original, magnetic, and non-magnetic De-S slag. Comparing the original to the magnetic De-S slag, the Fe content increased from 4.92 wt% to 9.46 wt% after the magnetic separation conducted in the laboratory, while the Ca content decreased from 40.15 wt% to 36.68 wt%. The non-magnetic De-S slag contained 42.44 wt% of Ca (~59 wt% as CaO), 14.86 wt% of Si (~32 wt% as SiO_2), and only 1.94 wt% of Fe. In terms of heavy metals, the concentrations of Cr, Ni, Cu, Zn, As, Cd, Hg, and Pb in the De-S slag were all below the detection limits. These findings indicate that the non-magnetic fraction of the De-S slag should be capable of partially replacing lime and silica sand for AAC production, and there is no concern about the risk of heavy metals when reusing it.

Fig. 2 shows the XRD patterns of the non-magnetic fraction of the De-S slag. Portlandite ($Ca(OH)_2$), calcite ($CaCO_3$), calcium silicate (γ-Ca_2SiO_4), quartz (SiO_2), graphite (C), and fluorite (CaF_2) are clearly observed, while some iron oxides, including Fe_2O_3 and Fe_3O_4, are present with a low diffraction intensity. Brand and Roesler [26] reported that free CaO often exists in steel slags because of the excess lime added in steelmaking, and it can cause the problem of volume expansion. However, it is noted that free CaO was not found in the non-magnetic fraction of the De-S slag used in this

Table 2
Physical and chemical characteristics of original, magnetic, and non-magnetic De-S slags.

Item		De-S slag		
		Original	Magnetic	Non-magnetic
Moisture content (wt%)		9.36	NA[b]	NA[b]
Ash content (wt%)		84.31 (93.01)[a]	NA[b]	NA[b]
LOI (wt%)		6.33 (6.99)[a]	NA[b]	NA[b]
Magnetic fraction[a] (wt%)		39.68	NA[b]	NA[b]
Non-magnetic fraction[a] (wt%)		60.32	NA[b]	NA[b]
Major element[a] (wt%)	Na	2.55	2.82	2.38
	Mg	0.66	0.72	0.62
	Al	2.69	3.17	2.38
	Si	15.43	16.92	14.86
	K	0.76	1.01	0.61
	Ca	40.15	36.68	42.44
	Fe	4.92	9.46	1.94

Heavy metals, including Cr, Ni, Cu, Zn, As, Cd, Hg, and Pb, were below the detection limits (<2 mg/kg).
[a] Dry basis.
[b] NA: not available.

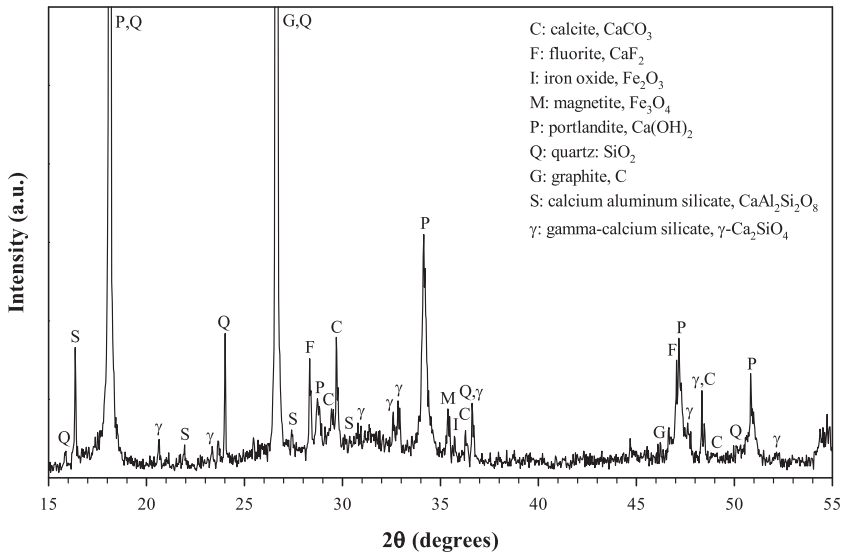

Fig. 2. XRD patterns of the non-magnetic fraction of De-S slag.

work. These results indicate that the lime added in the desulfurization process of steelmaking has been converted into other calcium compounds, namely $Ca(OH)_2$, $CaCO_3$, and γ-Ca_2SiO_4, and this may have an influence on the production of AAC. A little free CaO might exist when the slag was discharged from the steel mill, but it can quickly react with H_2O and CO_2 to form $Ca(OH)_2$ and $CaCO_3$ during cooling because of the fine particle size of the De-S slag. Generally, the non-magnetic fraction of De-S slag is rich in calcium and silicon compounds, and therefore should be suitable to be reused as an AAC raw material. In this study, after removing the magnetic substances, the non-magnetic fraction of the De-S slag was ground into powder <0.15 mm to be used as an alternative raw material in the subsequent experiments on AAC production.

3.2. Properties of AAC specimens produced with De-S slag

Fig. 3 presents the bulk density and compressive strength of the AAC specimens produced with 0–40 wt% of De-S slag. The reference specimen, which was produced without the De-S slag, had a bulk density of 673 kg/m^3 and a compressive strength of 6.59 MPa. When using the De-S slag as a raw material for AAC production, the bulk density of the AAC specimens slightly decreased from

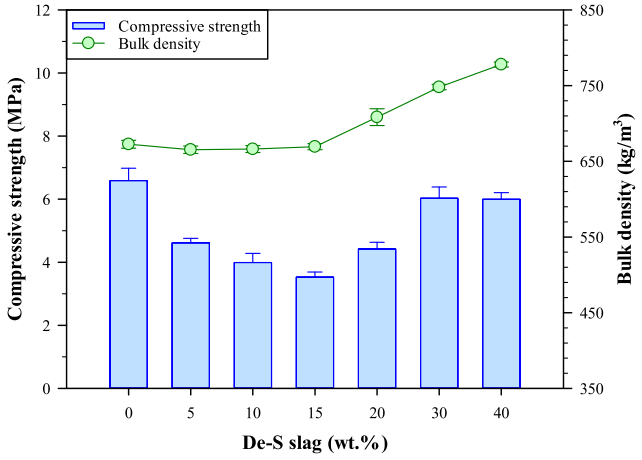

Fig. 3. Bulk density and compressive strength of the AAC specimens produced with De-S slag.

673 kg/m^3 to 669 kg/m^3 in the range of 0–15 wt% of the De-S slag, but with more slag added, it gradually increased to 778 kg/m^3. The variation in compressive strength of the AAC specimens was similar to that of the bulk density. The compressive strength decreased from 6.59 MPa to 3.53 MPa when 0–15 wt% of the De-S slag was added, and then reversed to increase to approximately 6 MPa. The bulk density and compressive strength of the AAC specimens usually depend on many factors, e.g. types of raw materials and their mix proportions, the water-solids ratio, types and quantity of a foaming agent, and autoclave curing conditions (temperature and time). It is typical for lightweight materials that the bulk density and compressive strength show the same variations. However, the tendency in this study (an increase following a decrease) is unusual, and there should be an influence exerted by the De-S slag. At low levels of De-S slag being added (0–15 wt%), the bulk density and compressive strength showed a tendency to decrease, a finding which is consistent with some previous studies [27,28]. Traditionally, lime is used for AAC production, and CaO will react with H_2O to form $Ca(OH)_2$ and generate much heat, thus significantly consuming the added water. In this study, the CaO in the De-S slag has mostly converted to $Ca(OH)_2$ and $CaCO_3$, and the consumption of water should decrease when using the De-S slag to replace lime. This therefore leaves more free water in the AAC mortars and reduces the bulk density and compressive strength. On the other hand, when the amount of De-S slag was further increased from 15 wt% to 40 wt%, we clearly observed that the foaming process was inhibited and the expansion of specimens was retarded. Consequently, the bulk density and compressive strength of the AAC specimens stopped decreasing and then inversely increased.

Fig. 4 shows the amount of gas generation with the AAC mortars prepared under different conditions. The foaming and expansion of AAC mortars rely on the hydrogen gas generated by the chemical reaction of aluminum under high alkaline conditions (see Eq. (2)). It is noted that the amount of gas generated was negatively correlated with the addition of De-S slag when using water for the preparation of AAC mortars. When the amount of the De-S slag added was increased, then the amount of gas generated fell continuously from 5.8 to 3.4 mL-gas/g-sample. These results indicate that the aluminum reaction was severely hindered at high levels of the De-S slag addition due to the insufficient alkalinity of the AAC mortars. In Table 1, the amount of lime addition was reduced as the amount of De-S slag was increased in order to keep the ratio of CaO/SiO_2 consistent. However, the calcium compounds in the

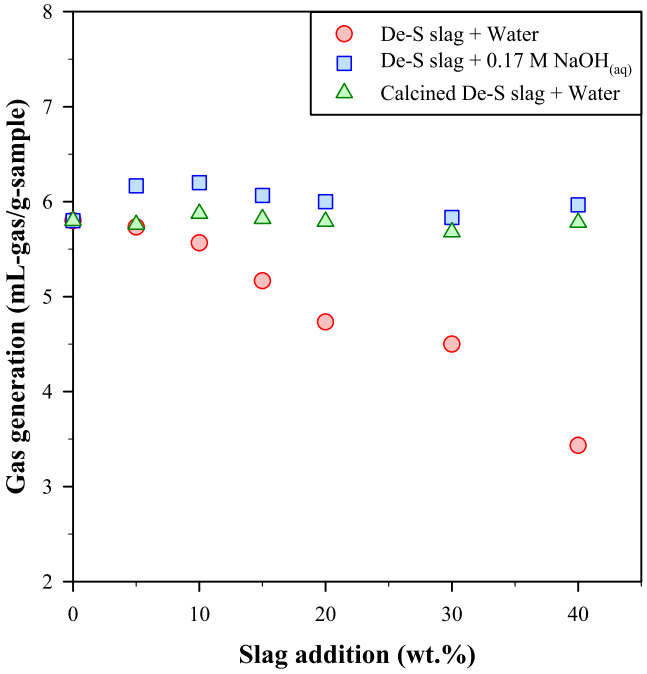

Fig. 4. Gas generation of different AAC mortars.

De-S slag were $Ca(OH)_2$, $CaCO_3$, γ-Ca_2SiO_4, and CaF_2 rather than CaO, so that the alkalinity of the resulting AAC mortars would decrease significantly. This is responsible for the retardation of the hydrogen gas generation. Without enough gas to expand the mortars, the bulk density and compressive strength of the AAC specimens was thus greatly increased.

$$2Al + 2OH^- + 6H_2O \rightarrow 2[Al(OH)_4]^- + 3H_2 \quad (2)$$

Two methods was tested in this study to address the low alkalinity of the mortars produced with the De-S slag: (1) replacing the added water with a 0.17 M aqueous solution of NaOH, and (2) calcining the De-S slag in advance. The non-magnetic fraction of the De-S slag was calcined at 900 °C for 1 h in order to decompose $Ca(OH)_2$ and $CaCO_3$ into CaO. The calcined De-S slag was then ground again to pass through a 0.15 mm sieve for AAC production. Fig. 4 also shows the gas generated by the AAC mortars prepared using these two methods. The amount of gas generated fluctuated between 5.8 and 6.2 mL-gas/g-sample when using 0.17 M $NaOH_{(aq)}$ to replace water, and similar results were observed when using the calcined De-S slag. These findings demonstrate that the chemical reaction of aluminum can proceed well under sufficient alkaline conditions and generate comparable amounts of hydrogen gas. Accordingly, the use of 0.17 M $NaOH_{(aq)}$ and the calcination of the De-S slag should both be capable of improving the foaming and expansion of the AAC mortars prepared with the De-S slag.

Fig. 5 presents the bulk density and compressive strength of the AAC specimens produced with 0–40 wt% of the De-S slag using 0.17 M $NaOH_{(aq)}$. Unlike Fig. 3, it was found that both the bulk density and compressive strength gradually decreased as the amount of the De-S slag was increased from 0 to 40 wt%. This indicates that once the foaming of AAC mortars is improved, the bulk density and compressive strength have a stable decreasing tendency. As well as the influence of the mineral composition of the De-S slag, the particle size of the slag may also affect the properties of the AAC specimens. In this study, the particle sizes of lime and silica were below 0.075 and 0.045 mm, respectively, while that of the De-S slag was below 0.15 mm. Różycka and Pichór [27] noted that the bulk density of AAC specimens was reduced due to the coarser perlite particles compared to ground quartz sand grains. Coarse particles theoretically have less specific surface area and adsorb less alkaline liquid on their surfaces than fine particles. Consequently, more alkaline liquid is free between particles, and this makes the mortars easier to expand and results in specimens of lower bulk density.

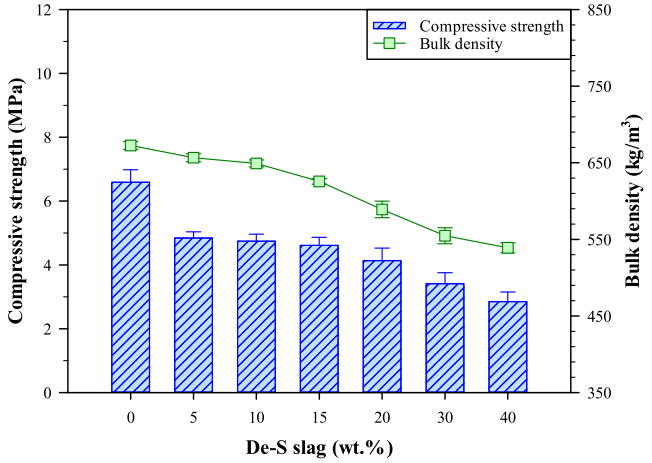

Fig. 5. Bulk density and compressive strength of the AAC specimens produced with De-S slag using 0.17 M NaOH(aq).

Fig. 6 shows the bulk density and compressive strength of the AAC specimens produced with the calcined De-S slag and water. During the preparation of AAC specimens, it was observed that the foaming and expansion of the mortars produced with the calcined De-S slag were adequate and stable. The bulk density of the resulting AAC specimens slightly increased first and then gradually declined as the amount of calcined De-S slag increased. Compared to Fig. 5, the bulk density is higher than that of the specimens prepared with 0.17 M $NaOH_{(aq)}$. On the other hand, the compressive strength had a tendency to decrease similar to that in Fig. 5, but its values were slightly higher for the same amount of slag that was added. The most likely explanation is that the CaO in the calcined De-S slag consumed some added water and reduced the actual water-solids ratios, thus increasing the bulk density and compressive strength of the AAC specimens.

Since the bulk density and compressive strength of the AAC specimens varied simultaneously, it was difficult to directly understand the effects on the properties of the AAC. Some previous

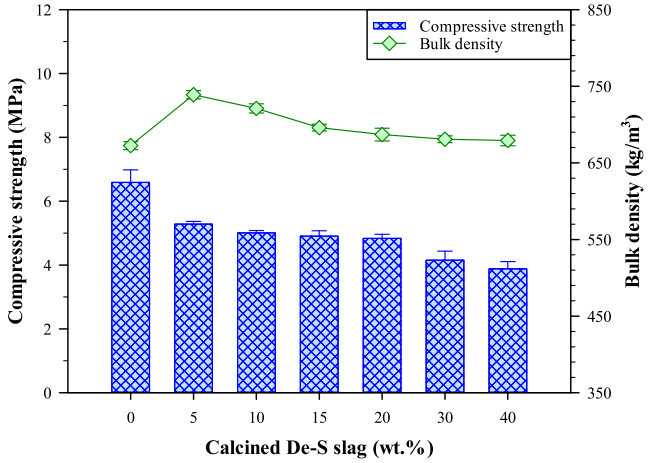

Fig. 6. Bulk density and compressive strength of the AAC specimens produced with calcined De-S slag using water.

studies [22,23,29] used a performance factor (P_f) to examine the variation in the relation between compressive strength and unit weight. The P_f value is defined as the proportion of compressive strength to unit weight, and can be regarded as the relative compressive strength provided by a lightweight material with a unit weight equal to 1000 kg/m^3. The P_f values of the AAC specimens produced under different conditions are presented in Fig. 7. Kurama et al. [23] produced AAC from coal bottom ash and showed that the P_f values of the products were between 2 and 5 MPa/1000-kg/m^3. Karakurt et al. [22] used natural zeolite to make AAC products that had P_f values in the range 1.5–6 MPa/1000-kg/m^3. In comparison, the P_f values of AAC specimens produced in this work were about 5–10 MPa/1000-kg/m^3, which are much higher than the previous studies. It is noteworthy that the P_f value of the AAC specimens produced with the De-S slag and water showed a large fluctuation. This means that the performance of the AAC products is very unstable. In contrast, when using the NaOH aqueous solution to replace water or calcining the De-S slag in advance, the P_f value of the AAC specimens presented a consistent tendency. These findings indicate that the stability in properties of the AAC specimens was significantly enhanced by adopting the foaming improvement methods presented in this work.

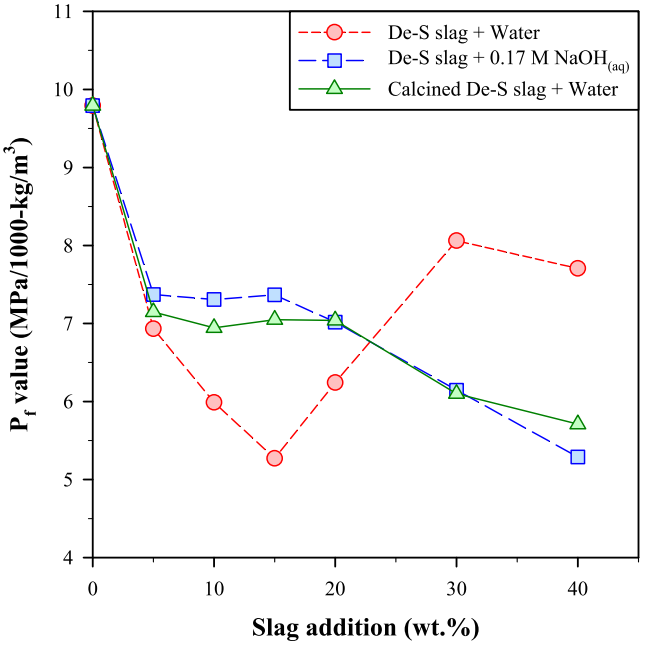

Fig. 7. Performance analysis of the AAC specimens.

Table 3
Physical requirements for AAC (ASTM C1693).

Strength class	Compressive strength (MPa)	Nominal dry bulk density (kg/m^3)	Density limits (kg/m^3)
AAC-2	2.0	400	350–450
		500	450–550
AAC-4	4.0	500	450–550
		600	550–650
		700	650–750
		800	750–850
AAC-6	6.0	600	550–650
		700	650–750
		800	750–850

Table 3 lists the physical requirements of AAC products described in ASTM C1693 [24]. By comparing the experimental results to the requirements, the classification of the AAC specimens is shown in Table 4. It was found that the AAC specimens produced with 10 and 15 wt% of the De-S slag and water failed to meet the requirements of any AAC class, but those produced with less or more De-S slag can achieve Class AAC-6 and/or Class AAC-4. On the other hand, the specimens produced with the De-S slag and 0.17 M $NaOH_{(aq)}$ were classified following the order of AAC-6, AAC-4, and then AAC-2, when an increasing amount of De-S slag was added. The AAC specimens produced with the calcined De-S slag and water also had a similar order in classification. The strength class of an AAC product went down from AAC-6 to AAC-2, as the amount of calcined De-S slag increased. In sum, without enhancing the alkalinity to improve the foaming of mortars, the properties of the AAC specimens produced with the De-S slag are unstable. This will create serious problems in AAC manufacturing and affect the quality of products. Using 0.17 M $NaOH_{(aq)}$ to replace water or calcining the De-S slag in advance can both solve the problem of insufficient alkalinity of mortars, and thus make the properties of AAC products more stable and predictable. This would make it easier to use De-S slag in AAC manufacturing. With regard to the issues of energy consumption, possible cost, and operation difficulty, we suggest that the use of a NaOH aqueous solution would be superior to calcining the De-S slag in advance.

3.3. Microstructures of the AAC specimens

Fig. 8 presents the results of thermal analysis for the AAC specimens produced with the De-S slag and 0.17 M $NaOH_{(aq)}$. By comparing the TG curves with DSC curves, two endothermic peaks accompanied by weight losses are observed at relatively low temperatures. The endothermic peak located around 450 °C is attributed to the decomposition of $Ca(OH)_2$, and the other one near 700 °C is related to the decarbonation of $CaCO_3$. Both $Ca(OH)_2$ and $CaCO_3$ can be regarded as unreacted calcium compounds persisting in the AAC specimens. The results shown in Fig. 8 indicate that small amounts of $Ca(OH)_2$ and $CaCO_3$ were present in the AAC specimens, whether or not the De-S slag was used. In addition to the endothermic peaks, an exothermic peak without weight loss was found between 800 and 900 °C. Yang et al. [30] studied the phase transition of tobermorite at elevated temperatures, and noted that tobermorite can progressively convert to wollastonite ($CaSiO_3$) and an exothermic peak without weight loss appears at 861 °C. In this

Table 4
Classification of the AAC products prepared under different conditions.

Slag amount (wt%)	De-S slag + Water	De-S slag + 0.17 M $NaOH_{(aq)}$	Calcined De-S slag + Water
0	AAC-4, AAC-6	AAC-4, AAC-6	AAC-4, AAC-6
5	AAC-4	AAC-4	AC-4
10	–	AAC-4	AC-4
15	–	AAC-4	AC-4
20	AAC-4	AAC-4	AC-4
30	AAC4, AAC-6	–	AC-4
40	AAC-4	AAC-2	–

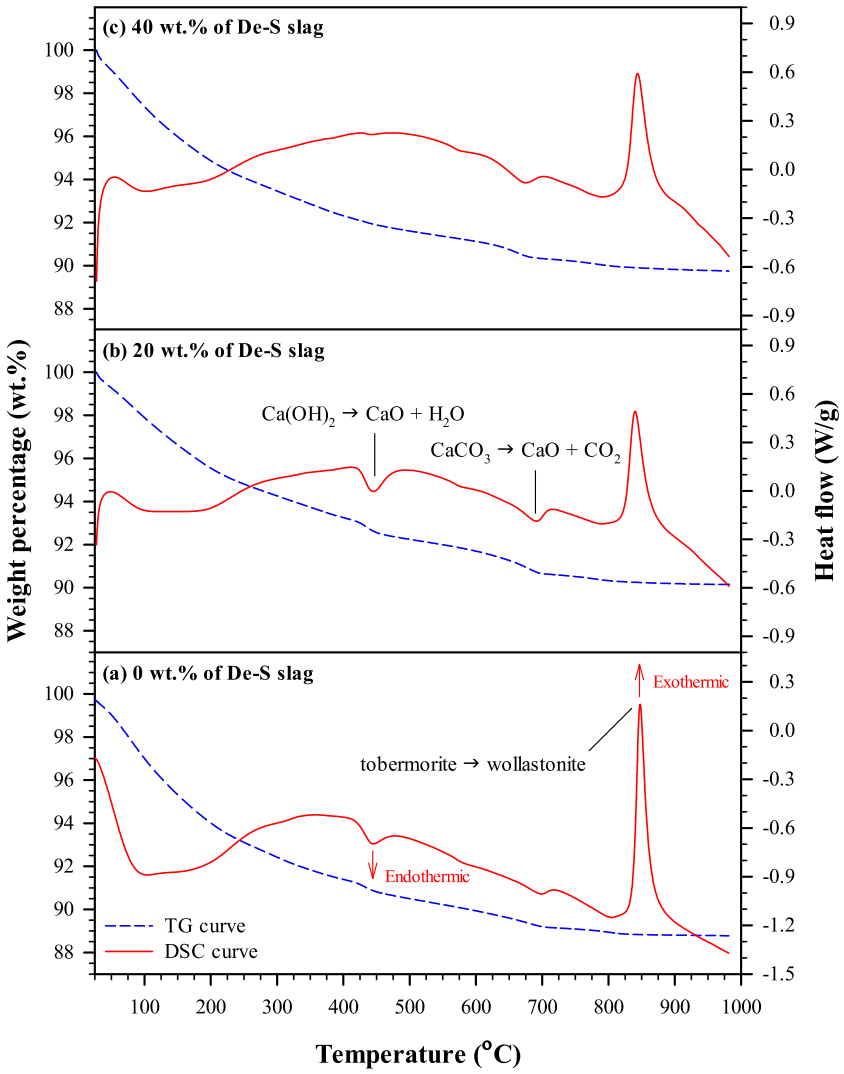

Fig. 8. TG and DSC curves of AAC specimens produced with (a) 0 wt%, (b) 20 wt%, and (c) 40 wt% of De-S slag using 0.17 M NaOH(aq).

study, the exothermic peak related to tobermorite became less significant when increasing the amount of De-S slag. The results show that the formation of tobermorite was hindered due to the addition of De-S slag. The foreign ions introduced by the De-S slag, such as Na^+, K^+, Mg^{2+}, and Al^{3+}, may be responsible for the influence on the tobermorite formation. Mostafa [21] produced AAC from air-cooled slag, which also contained Na_2O, K_2O, MgO, Al_2O_3, and other foreign ions, and it was indicated that the formation of tobermorite was retarded due to the addition of slag. Furthermore, Connan et al. [31] noted that the size of the exothermic peak was closely correlated to the compressive strength. This could be a partial explanation for the reduction in compressive strength that was observed above.

Fig. 9 shows the SEM images of the AAC specimens produced with 0 wt%, 20 wt%, and 40 wt% of De-S slag using 0.17 M $NaOH_{(aq)}$. In the reference specimen (Fig. 9a), which was produced without the De-S slag, the tobermorite existed as lath-like structures. In contrast, in the AAC specimen produced with 20 wt% of the De-S slag (Fig. 9b), platy and fiber-like structures of tobermorite were observed. In comparison, the tobermorite changed to leafy structures when using 40 wt% of the De-S slag for the AAC production (Fig. 9c). Some studies reported that the morphology of tobermorite changed due to the presence of foreign ions. Mostafa et al. [32] reported that fiber-like tobermorite was found when iron ions substituted for silicate ions in the tobermorite structure. Mostafa et al. [33] studied the synthesis and characterization of tobermorite, and indicated that sulfate ions increased the crystalline imperfection of tobermorite, thus resulting in leafy tobermorite. When reusing the De-S slag as a raw material for AAC production, some impurities, such as iron and sulfate ions, can be introduced into the AAC specimens, and this could therefore affect the morphological features of tobermorite. Moreover, Różycka, and Pichór [27] suggested that a reduction in the compressive strength of AAC might be related to the alteration in the morphology of tobermorite. Lath-like tobermorite crystals provided higher compressive strength for the AAC specimens made from perlite waste [27]. As the amount of the perlite waste was increased up to 40 wt%, the tobermorite changed to small, grass-like structures and the compressive strength of the AAC specimens fell significantly [27]. In this study, the reduction in the compressive strength of the AAC specimens produced with De-S slag should be attributed not only to the interference in the tobermorite formation, but also the alteration in the tobermorite morphology.

4. Conclusions

The following conclusions can be drawn from the present work. The non-magnetic fraction accounted for ~60 wt% of the De-S slag

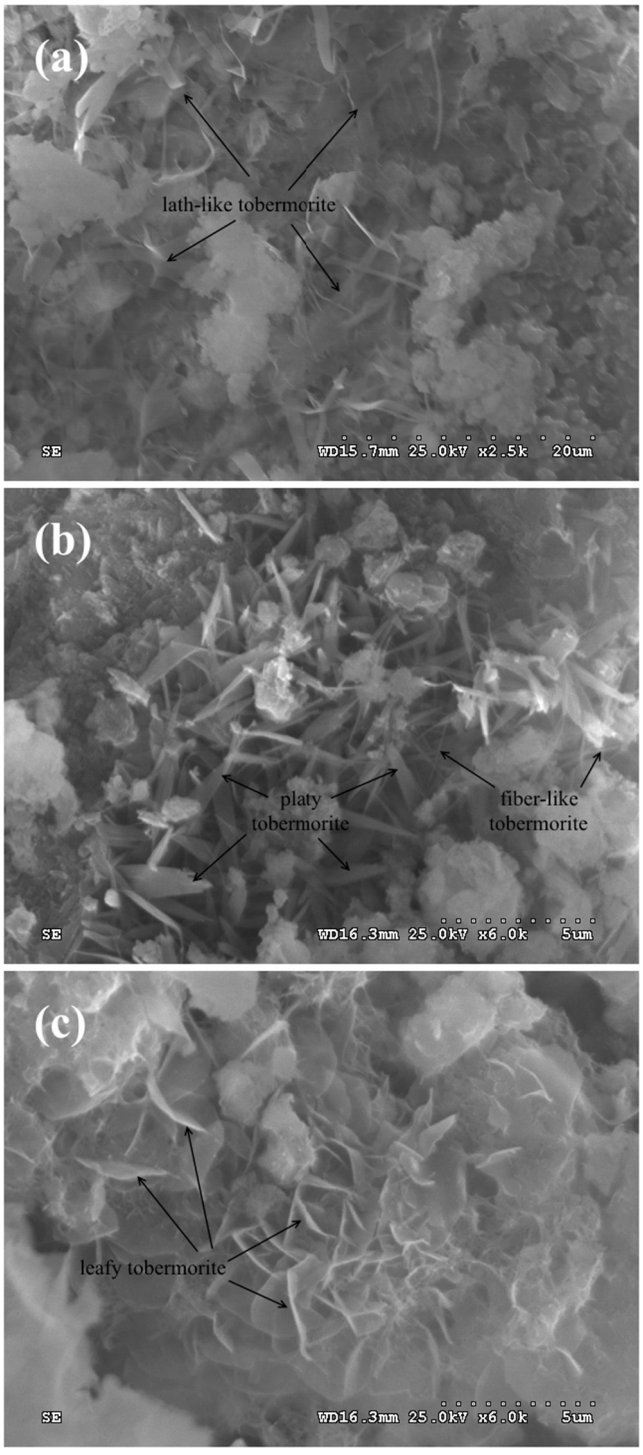

Fig. 9. SEM images of the AAC specimens produced with (a) 0 wt%, (b) 20 wt%, and (c) 40 wt% of De-S slag using 0.17 M NaOH(aq).

and was mainly composed of Ca and Si compounds; it should thus be suitable to replace lime and silica sand for AAC production. The concentrations of heavy metals in the De-S slag were all below the detection limits, which means that the environmental risk of reusing the De-S slag is insignificant. The calcium compounds in the De-S slag were $Ca(OH)_2$, $CaCO_3$, γ-Ca_2SiO_4, and CaF_2 rather than CaO, and this may influence the AAC production. When using the De-S slag and water to produce AAC specimens, both the bulk density and compressive strength initially decreased as the amount of the De-S slag increased (0–15 wt%), but then reversed and increased when more slag was added. When the amount of the De-S slag added was over 15 wt%, then the inhibition of foaming was observed during the AAC production, due to the insufficient alkalinity of the mortars. The results with regard to gas generated by the AAC mortars further confirmed the effects of insufficient alkalinity on the foaming and expansion of the mortars. By using 0.17 M $NaOH_{(aq)}$ to replace water or calcining the De-S slag in advance, the problem of foaming was improved and the mortars can expand sufficiently. The bulk density and compressive strength of the resulting AAC specimens thus showed a consistent decreasing tendency. After improving the foaming of mortars, the AAC products had predicable properties and their quality became more stable. In consideration of the energy consumption, possible cost, and operation difficulty, it is suggested that using 0.17 M $NaOH_{(aq)}$ to replace water would be superior to calcining the De-S slag in advance. The formation and morphology of tobemorite were affected by the addition of De-S slag, which is probably due to the foreign ions introduced by the slag. The effects on tobermorite in the AAC specimens should partially responsible for the reduction in compressive strength.

Acknowledgements

The authors gratefully acknowledge the Ministry of Science and Technology, Taiwan, for its financial support of this study (Contract No.: MOST 106-3114-E-006-007 and MOST 106-3113-E-007-002).

References

[1] E.T. Turkdogan, Fundamentals of Steelmaking, Institute of Materials, London, 1996.
[2] G. Sheng, P. Huang, S. Wang, G. Chen, Potential reuse of slag from the Kambara reactor desulfurization process of iron in an acidic mine drainage treatment, J. Environ. Eng. 140 (7) (2014).
[3] S.K. Kawatra, S.J. Ripke, Pelletizing steel mill desulfurization slag, Int. J. Miner. Process. 65 (3–4) (2002) 165–175.
[4] Y.-L. Chen, J.-E. Chang, P.-H. Shih, M.-S. Ko, Y.-K. Chang, L.-C. Chiang, Reusing pretreated desulfurization slag to improve clinkerization and clinker grindability for energy conservation in cement manufacture, J. Environ. Manage. 91 (9) (2010) 1892–1897.
[5] C. Loper Jr, J. Kristiansen, A. Haase, R. Bigge, F. Quilling, Beneficial reuse of desulfurization slag, Trans. Am. Foundrymen's Soc. 104 (1996) 29–32.
[6] J.I. Bhatty, J. Gajda, Alternative materials: pyroprocessing, World Cem. 35 (12) (2004) 41–48.
[7] N. Ma, J.B. Houser, Recycling of steelmaking slag fines by weak magnetic separation coupled with selective particle size screening, J. Clean Prod. 82 (2014) 221–231.
[8] W.-T. Kuo, H.-Y. Wang, C.-Y. Shu, Engineering properties of cementless concrete produced from GGBFS and recycled desulfurization slag, Constr. Build. Mater. 63 (2014) 189–196.
[9] J.Y. Hwang, Verification of Steelmaking Slags Iron Content – Final Technical Progress Report, Michigan Technological University, Houghton, MI, 2006.
[10] C.-L. Ho, W.-L. Huang, H.-Y. Wang, Study of the volume stability of slag cement mortar applied to desulfurization slag during high temperature operation, Constr. Build. Mater. 144 (2017) 147–157.
[11] L.-J. Huang, H.-Y. Wang, C.-T. Wei, Engineering properties of controlled low strength desulfurization slags (CLSDS), Constr. Build. Mater. 115 (2016) 6–12.
[12] D.-H. Shen, C.-M. Wu, J.-C. Du, Laboratory investigation of basic oxygen furnace slag for substitution of aggregate in porous asphalt mixture, Constr. Build. Mater. 23 (1) (2009) 453–461.
[13] G. Wang, Determination of the expansion force of coarse steel slag aggregate, Constr. Build. Mater. 24 (10) (2010) 1961–1966.
[14] G. Wang, Y. Wang, Z. Gao, Use of steel slag as a granular material: volume expansion prediction and usability criteria, J. Hazard. Mater. 184 (1–3) (2010) 555–560.
[15] L. Cai, B. Ma, X. Li, Y. Lv, Z. Liu, S. Jian, Mechanical and hydration characteristics of autoclaved aerated concrete (AAC) containing iron-tailings: effect of content and fineness, Constr. Build. Mater. 128 (2016) 361–372.
[16] A.J. Hamad, Materials, production, properties and application of aerated lightweight concrete: review, Int. J. Mater. Sci. Eng. 2 (2) (2014) 152–157.
[17] N. Narayanan, K. Ramamurthy, Structure and properties of aerated concrete: a review, Cem. Concr. Compos. 22 (5) (2000) 321–329.
[18] K. Matsui, J. Kikuma, M. Tsunashima, T. Ishikawa, S.-Y. Matsuno, A. Ogawa, M. Sato, In situ time-resolved X-ray diffraction of tobermorite formation in autoclaved aerated concrete: Influence of silica source reactivity and Al addition, Cem. Concr. Res. 41 (5) (2011) 510–519.

[19] S.Y. Hong, F.P. Glasser, Phase relations in the CaO–SiO_2–H_2O system to 200 °C at saturated steam pressure, Cem. Concr. Res. 34 (9) (2004) 1529–1534.
[20] X.-Y. Huang, W. Ni, W.-H. Cui, Z.-J. Wang, L.-P. Zhu, Preparation of autoclaved aerated concrete using copper tailings and blast furnace slag, Constr. Build. Mater. 27 (1) (2012) 1–5.
[21] N.Y. Mostafa, Influence of air-cooled slag on physicochemical properties of autoclaved aerated concrete, Cem. Concr. Res. 35 (7) (2005) 1349–1357.
[22] C. Karakurt, H. Kurama, İ.B. Topçu, Utilization of natural zeolite in aerated concrete production, Cem. Concr. Compos. 32 (1) (2010) 1–8.
[23] H. Kurama, İ.B. Topçu, C. Karakurt, Properties of the autoclaved aerated concrete produced from coal bottom ash, J. Mater. Process. Technol. 209 (2) (2009) 767–773.
[24] ASTM, C1693-11, Standard Specification for Autoclaved Aerated Concrete (AAC), ASTM International, West Conshohocken, PA, 2011.
[25] N. Menad, N. Kanari, M. Save, Recovery of high grade iron compounds from LD slag by enhanced magnetic separation techniques, Int. J. Miner. Process 126 (2014) 1–9.
[26] A.S. Brand, J.R. Roesler, Steel furnace slag aggregate expansion and hardened concrete properties, Cem. Concr. Compos. 60 (2015) 1–9.
[27] A. Różycka, W. Pichór, Effect of perlite waste addition on the properties of autoclaved aerated concrete, Constr. Build. Mater. 120 (2016) 65–71.
[28] K. Kunchariyakun, S. Asavapisit, K. Sombatsompop, Properties of autoclaved aerated concrete incorporating rice husk ash as partial replacement for fine aggregate, Cem. Concr. Compos. 55 (2015) 11–16.
[29] S.K. Lim, C.S. Tan, X. Zhao, T.C. Ling, Strength and toughness of lightweight foamed concrete with different sand grading, KSCE J. Civil Eng. 19 (7) (2015) 2191–2197.
[30] X. Yang, C. Cui, X. Cui, G. Tang, H. Ma, High-temperature phase transition and the activity of tobermorite, J. Wuhan Univ. Technol.-Mater. Sci. Ed. 29 (2) (2014) 298–301.
[31] H. Connan, D. Klimesch, A. Ray, P. Thomas, Thermal characterisation of autoclaved cement made with alumina-silica rich industrialwaste, J. Therm. Anal. Calorim. 84 (2) (2006) 521–525.
[32] N.Y. Mostafa, E.A. Kishar, S.A. Abo-El-Enein, FTIR study and cation exchange capacity of Fe^{3+}- and Mg^{2+}-substituted calcium silicate hydrates, J. Alloys Compd. 473 (1–2) (2009) 538–542.
[33] N.Y. Mostafa, A.A. Shaltout, H. Omar, S.A. Abo-El-Enein, Hydrothermal synthesis and characterization of aluminium and sulfate substituted 1.1 nm tobermorites, J. Alloys Compd. 467 (1–2) (2009) 332–337.